

Physically based cold regions river flood prediction in data-sparse regions: The Yukon River Basin flow forecasting system

Mohamed Elshamy^{1,2}  | Youssef Loukili^{1,2} | John W. Pomeroy¹ |
Alain Pietroniro^{1,3,4} | Dominique Richard¹ | Daniel Princz³

¹Centre for Hydrology, University of Saskatchewan, Saskatoon, Saskatchewan, Canada

²Global Institute for Water Security, University of Saskatchewan, Saskatoon, Saskatchewan, Canada

³National Hydrological Service, Environment and Climate Change Canada, Saskatoon, Saskatchewan, Canada

⁴Department of Civil Engineering, University of Calgary, Calgary, Alberta, Canada

Correspondence

Mohamed Elshamy, Centre for Hydrology, University of Saskatchewan, Saskatoon, SK, Canada.

Email: mohamed.elshamy@usask.ca

Funding information

Global Water Futures; Yukon Environment

Abstract

The Yukon River Basin (YRB) is one of the most important river networks shared between Canada and The United States, and is one of the largest river basins in the subarctic region of North America. The Canadian part of the YRB is characterized by steeply sloped, partly glaciated mountain headwaters that generate considerable runoff during melt of glaciers and seasonal snow-cover. Snow redistribution, snowmelt, glacier melt and freezing–thawing soil processes in winter and spring along with summertime rainfall–runoff and evapotranspiration processes are thus key components of streamflow generation in the basin, making conceptual rainfall–runoff models unsuitable for this cold region. Due to the remote high latitudes and high altitudes of the basin, there is a paucity of observational data, making heavily calibrated conceptual modeling approaches infeasible. At the request of the Yukon Government, this project developed and operationalized a streamflow forecasting system for the Yukon River and several of its tributary rivers using a distributed land surface modeling approach developed for large-scale implementation in cold regions. This represents a substantial advance in bringing operational hydrological forecasting to the Canadian subarctic for the first time. This experience will inform future research to operation improvements as Canada develops a nationally coordinated flood forecast system.

KEYWORDS

flood generation, forecasting and warning, hydrological modeling

1 | INTRODUCTION

The prohibitive costs of flood disasters in terms of life and property losses and acute human stresses, have urged

scientists, governments, and organizations to encourage the development of a new generation of flood forecasting systems that incorporate advances in hydrometeorological and hydrological modeling, computing and

This is an open access article under the terms of the [Creative Commons Attribution-NonCommercial-NoDerivs](https://creativecommons.org/licenses/by-nc-nd/4.0/) License, which permits use and distribution in any medium, provided the original work is properly cited, the use is non-commercial and no modifications or adaptations are made.

© 2022 The Authors. *Journal of Flood Risk Management* published by Chartered Institution of Water and Environmental Management and John Wiley & Sons Ltd.

hydroinformatics with improvement in observational technologies. As Perera et al. (2019) stated, the direct quantification of benefits from Flood Early Warning Systems (FEWS) is difficult but can be indirectly assessed by correlating the number of established systems during 2000–2017 and the reported reduction in damages and loss of life from flooding during the same period by the Centre for Research on Epidemiology of Disasters Emergency Events Database—CRED's EM-DAT (<https://www.emdat.be>). The number of established FEWS in 2000–2017 accounted for 50% of the surveyed systems (Perera et al., 2019) indicating the level of effort exerted worldwide since the turn of the 21st century. Cold regions are indeed prone to flooding threats of different types, and the incorporation of snow hydrology models into some FEWS has helped to better predict and manage snowmelt floods. For instance, in spring 1993, the Watershed Simulation and Forecasting System (WSFS) developed in Finland (Vehvilainen & Huttunen, 2001) saved around 5 million Finnish Marks of damage cost by informing appropriate operating rules for regulated lakes at the northern River Kemijoki. A popular flood forecasting software framework is Delft-FEWS, which was introduced as an open shell that can flexibly integrate models and data (Werner & van Dijk, 2005). The latest overview map of Delft-FEWS (<https://fewsappliances.netlify.app>) indicates 126 flood forecasting applications worldwide. This is only one software system, many other FEWS do not necessarily utilize that software, but the number is indicative of the developments of forecasting systems worldwide.

Arduino et al. (2005) synthesized scientific and technological efforts by 150 presenters at the International Conference on Flood Forecasting in Europe (Rotterdam, 3–5 March 2003). They categorized them into precipitation forecasts, coupling precipitation forecasts with hydrological models, data-driven and process-based hydrological models, predictive uncertainty and flood risk assessments, and operational flood forecasting linked to flood warning dissemination. For cold regions, Gelfan and Motovilov (2009) provided a historical review and a summary of recent improvements of long-term hydrological forecasting methods practiced in the former USSR, the United States, Canada, and Scandinavia, with a focus on Russian methods. More recently, Zahmatkesh et al. (2019) reported in detail on operational flood forecasting as practiced in Canadian Provinces. Modeling methods have evolved from simple index and physical–statistical models, to semi-distributed and distributed hydrological models which are complex and not often successful in operational mode. Another review of river forecasting methods in cold regions and ungauged basins by Belvederesi et al. (2022) noted that regionalization, calibration,

and interpolation or regression are the main approaches to cope with limited data availability in remote cold regions. In a larger context presenting challenges surrounding floods and droughts prediction, Brunner et al. (2021) touched likewise upon the problem of limited data as the most important restriction, categorized it into eight main issues and suggested some tractable ways to address the problem.

The operationalization of a streamflow forecasting system in data-sparse cold regions does not lend itself to standard hydrological modeling practice. Sparse monitoring infrastructure, due to its high cost and the remoteness of the region, requires a different forecasting approach that uses a blend of more traditional forecasting approaches and detailed process-based understanding based on physically based models to achieve the desired result. The modeling system used in the development of the Yukon operational forecasting system presented here is one that has had a long history of development within Canada and was deemed appropriate for this domain given its unique cold-regions aspects, physical basis, and the scarcity of streamflow observations to calibrate models. The modeling system is the MESH hydrology land-surface model whose development began in Canada in the 1990s (Soulis et al., 2000) with the World Climate Research Programme's Global Energy and Water Experiment (GEWEX) and its regional hydroclimate study, the Mackenzie GEWEX Study (MAGS). The focus at the time was the coupling of land surface schemes (LSS), common in Global Circulation Models (GCMs), to hydrological models (Pietroniro et al., 2001; Pietroniro & Soulis, 2003). The result culminated in the MESH framework (Pietroniro et al., 2007). Since its inception, MESH has been adapted to incorporate important cold regions hydrological processes and specifically those considered necessary for simulations in subarctic hydrological environments. Important considerations in choosing this H-LSM was its ability to deal with snow, glaciers, and the dominant processes required to maintain model fidelity, deal with sub-grid heterogeneity, and include important hydrological controls such as glaciers (Wheater et al., 2022).

There has been the perception amongst flood forecasters that research models are unsuitable for operations, partly due to their complexity and partly due to that they are computationally too expensive for large domains in real-time operational settings. There is also the argument that prediction in ungauged basins requires physically based process hydrology methods to constrain parameter uncertainty and model uncertainty (Pomeroy et al., 2004, 2013). The purpose of this study is, therefore, to demonstrate the feasibility of adopting a hydrological land surface model to forecast river discharge and peak streamflow in the Canadian subarctic. Specifically, it

aims to develop, parameterize, validate, and operationalize a discharge forecast support system for the Yukon River and several of its tributary rivers within the Yukon Territory, Canada. This effort requires a model capable of simulating the dominant hydrological processes in this cold region. The Yukon is one of the regions of Canada most impacted by climate change (Bush & Lemmen, 2019). The seasonal snowcover start, end, and duration are found to be sensitive to warming in the subarctic Yukon (Rasouli et al., 2021), confirming the need for a robust high fidelity model. Often, “physically-based” models in hydrology require computationally expensive and non-trivially convergent optimization of parameters (Clark et al., 2016; Kirchner, 2006). Therefore, the approach here tries to minimize the calibration burden by parameterizing the model from the results of advancements in hydrological science in the region, particularly the long-studied Wolf Creek Research Basin (Janowicz et al., 2004; Pomeroy et al., 2006; Pomeroy & Granger, 1999) and parameters that can be chosen from soil and biophysical inventories or remote sensing imagery. In this application, years of effort in developing models, including many years of observations and process experiments in Wolf Creek have allowed for parameterization of models based on the best-available science and experience in the region.

2 | MODELING DOMAIN AND METHODS

2.1 | The modeling domain

The Yukon River Basin is the fifth largest basin in North America with an area of more than 850,000 km², about 324,000 km² of which lies in Canada. The river originates at the Llewellyn Glacier in northwest British Columbia (BC) and flows northwest then west/southwest along a 3185 km course to discharge into the Bering Sea through the Yukon–Kuskokwim Delta (Figure 1 inset). The Yukon River and its tributaries cross impressive physiographic landscapes, as mapped by Brabets et al. (2000) with extremely to moderately high rugged mountains, high elevation icefields, rolling low mountains, rolling topography and gentle slopes, plains, and lowlands. The St. Elias Icefield in the SW Yukon headwaters is the largest continental icefield in the world after Greenland and Antarctica and has elevations up to 4700 m.a.s.l. (Figure 1). Many important lakes and wetlands in the basin add complexity to the Yukon River system. The part of the YRB considered here is gauged at Eagle (288,000 km²) and does not include the Canadian northern Porcupine River Basin. This basin is large, with its area exceeding that of the United Kingdom by 19%.

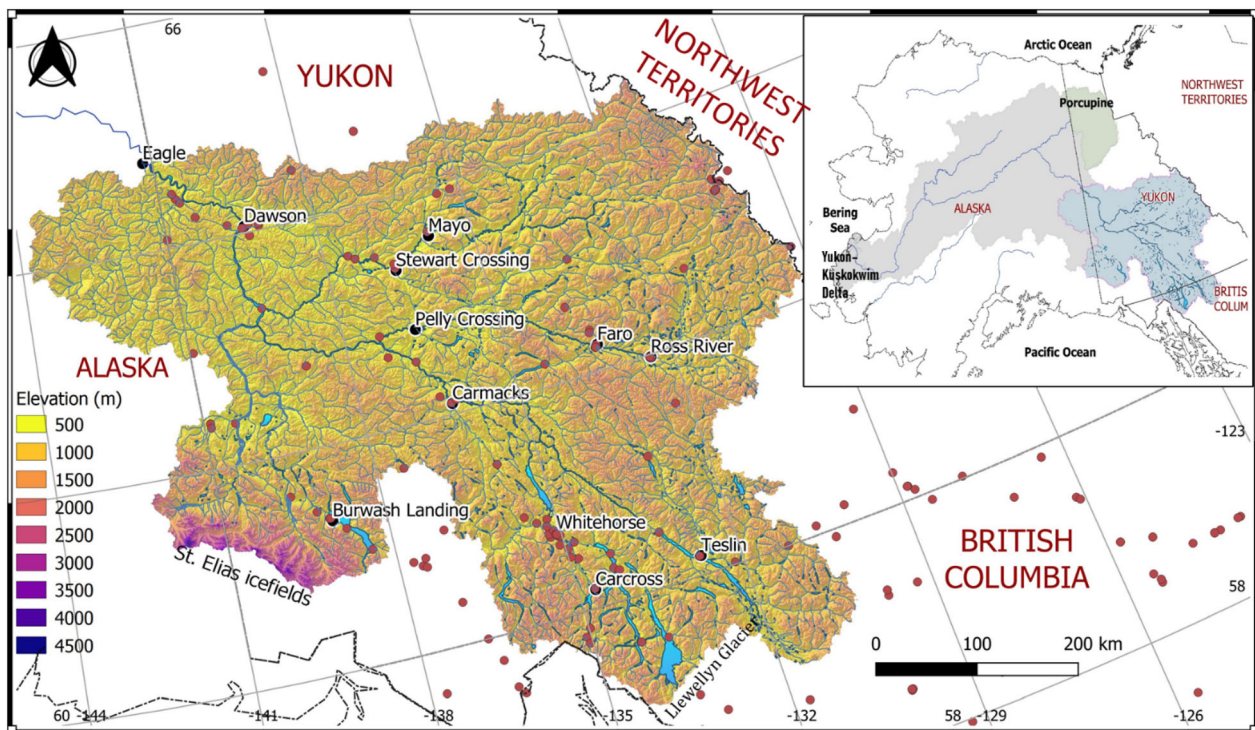


FIGURE 1 Digital elevation model of the Yukon River Basin at Eagle. Main cities/towns (black dots) and meteorological network (red dots) are also shown. Inset shows the basin location within the entire Yukon River Basin.

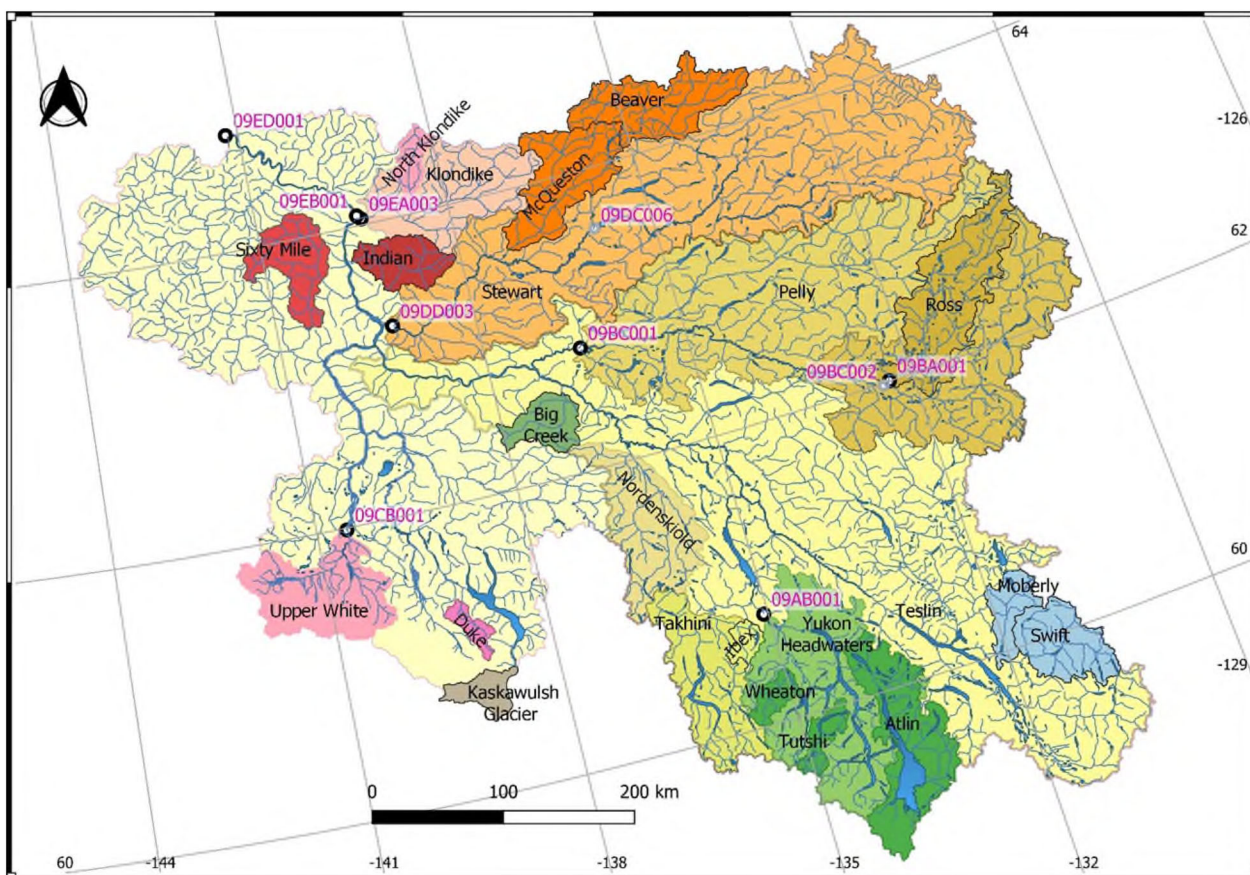


FIGURE 2 YRB@Eagle sub-basins (colored polygons) and forecast points (black circles for main points and smaller gray ones for secondary points) labeled using their Water Survey Canada (WSC) gauge IDs—further details in Table 3.

The YRB at Eagle, AK (hereafter YRB@Eagle), lies mainly within the Boreal Cordillera terrestrial ecozone except for narrow northern and eastern strips, located in the Taiga Cordillera (Smith et al., 2004). Soil categories include rough Alpine land in mountains, Brunisols in the majority of the domain, Cryosols toward the north and west, and Podzols in few areas in the south (Brabets et al., 2000). Drainage in the seasonally thawed active layer above permanently frozen ground, permafrost, is generally poor due to factors such as shallow soils, fine soil texture, and the presence of ice under the topsoil.

The climate of the Yukon River basin is continental, influenced by mountain topography and characterized by high seasonality expressed as long cold winters and short warm summers. Annual mean daily temperatures range between -2°C around Whitehorse to colder than -15°C in the St Elias Mountains at the headwaters of the White River (Wahl, 2004). January and July mean daily temperature ranges are -30°C to -15°C and -5°C to 15°C , respectively. Total annual precipitation varies substantially and is controlled by orography. The normal snow season spans from October to May, but at very high elevations, snow may fall throughout the year and

accumulate to contribute to glaciers. Solar irradiance and air temperature are the principal drivers of snow/ice melt and runoff amounts. According to Wahl et al. (1987), Jones and Fahl (1994), and Brabets et al. (2000), mean annual precipitation can exceed 1300 mm over the eastern slopes of St. Elias Icefields of the White River headwaters and Llewellyn Glacier of the Yukon Headwaters. Lower precipitation amounts, between 300 and 750 mm, fall over most of the basin, except for a corridor north of Whitehorse, YT which is downwind of high mountains and receives only 200–300 mm annually. It should be noted that the YRB@Eagle has a low density of unevenly distributed meteorological stations (Figure 1), with about 1 station per 3000 km^2 .

Streamflow from May to September stems from a combination of snowmelt, glacier melt and summer rain-storm runoff modulated by the storage and outflow from a system of large lakes in the Yukon Headwaters and Teslin River sub-basins (Figure 2). The southern Yukon Headwaters sub-basin has a total lake area of about 1320 km^2 . Maximum outflow from this system is reached in July/August if unregulated or August/September under controlled conditions for energy production.

TABLE 1 Spatial datasets used to build the MESH model for YRB@Eagle

Dataset	Source/description	Resolution	References
Digital Elevation Model (DEM)	Hydrologically conditioned MERIT-hydro	3 arc-s (~90 m)	Yamazaki et al. (2019)
Land Use/Cover	2010 Land Cover of North America based on LANDSAT v1.0	30 m	CCRS et al. (2017)
Soil Texture	Global Soil Database for Earth system modeling (GSDE)	1 km	Shangguan et al. (2014)
Climatic Forcing	Global Multiscale Model (GEM-RDPS), precipitation replaced by the Canadian Precipitation Analysis (CaPA) as available	10 km 1 h for GEM 6 h for CaPA	Côté et al. (1998) Mahfouf et al. (2007)

Brabets and Walvoord (2009) studied the streamflow trends in the YRB over the period 1944–2005 and found that annual discharges have remained relatively unchanged except for a few glacier-fed rivers that manifested increasing trends due to enhanced glacier melting. They also showed a high level of correlation in streamflow pattern changes with the Pacific Decadal Oscillation (PDO) where warm episodes are usually associated with above average winter flows and vice versa.

2.2 | The MESH modeling system

MESH is a community hydrological land surface modeling (H-LSM) framework coupling the Canadian Land Surface Scheme (CLASS; Verseghy, 2012), with a two-dimensional horizontal routing component (WATROUTE) adopted from the distributed hydrological model WATFLOOD (Kouwen, 1988). The LSM component aims to simulate the vertical processes of heat and moisture flux transfers between the land surface and the atmosphere. Unlike many LSMs, the vertical column in MESH has a topographic slope that allows for lateral transfer of overland flow and interflow (Soulis et al., 2000) to an assumed stream within each grid cell of the model before it is routed through the river network. CLASS includes the cold regions hydrology physical descriptions such as blowing snow transport and sublimation, snow interception and sublimation, energy balance snowmelt, influence of canopy on sub-canopy snowmelt, and water movement in partially frozen soils (Pomeroy et al., 1998).

MESH typically uses a regular latitude–longitude grid and represents sub-grid heterogeneity using the grouped response unit (GRU) approach (Kouwen et al., 1993). In this approach, a GRU in different grid cells shares the same set of parameters, which simplifies basin characterization and model parameterization. While land cover classes are usually used to define GRUs, other factors can be included in their definition such as soil type, slope, and aspect. MESH has been widely used in Canada to

study the Great Lakes Basin (Haghnegahdar et al., 2015) and the Saskatchewan River Basin (Yassin et al., 2017; Yassin, 2019) amongst others. Additional information is provided in Section S1. A full description of CLASS physics is given by Pomeroy et al. (2016) while Wheater et al. (2022) provide an account of recent MESH developments and applications.

3 | MESH MODEL DEVELOPMENT FOR THE YRB

The complex interdependency of geospatial information, observations and models requires systematic approaches for large scale modeling. Pre-processing of the network topology, land-use information, and driving meteorological data are required for basin discretization and model development. Figure 3 shows a general workflow for developing a MESH model setup where stage 1 (top) deals with model delineation and discretization and stage 2 (bottom) focuses on model parameterization. The YRB MESH model is the backbone of the forecasting system and therefore its development is described briefly below.

3.1 | Delineation and discretization

Physiographic geospatial information is readily available from public data sets as highlighted in Table 1. The YRB@Eagle was delineated—with Eagle AK (USGS 15356000, WSC 09ED001) as the natural outlet based on the hydrologically corrected MERIT-hydro DEM (Yamazaki et al., 2019) (Figure 1). The basin (288,000 km²) was discretized using a regular latitude–longitude grid at a spatial resolution of 0.125° (~10 km), matching that of the climatic forcing data used for model development (see below). This yielded a drainage database for the domain with 120 columns, 56 rows, and 3448 active grid cells. The initial drainage database contained attributes describing cell areas, flow directions, and slope and length of channels connecting

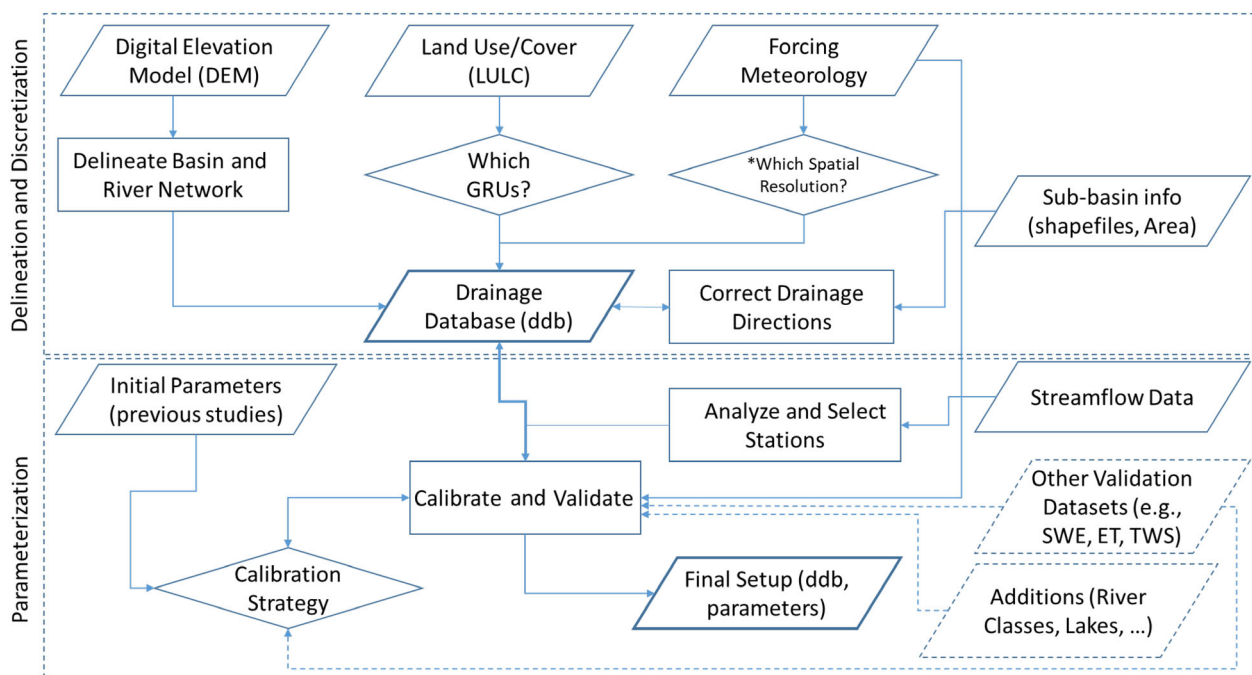


FIGURE 3 MESH model development workflow (dashed shapes/connectors indicate optional datasets that may be used; double-directional arrows indicate iterative procedures).

those cells based on elevations at the selected grid resolution. Additional fields were later added to improve river and lake routing as described in the next section.

GRUs were defined by land cover classes. There is a strong correlation between natural vegetation cover and sub-surface soil texture, drainage, permafrost, and geology in the region (Carey & Woo, 2001) which makes land cover classification a suitable determinant for GRU classification in the absence of soil surveys. The 2010 North American Land Cover (NALC; CCRS et al., 2017) remote sensing derived land cover classification was used for this purpose. The database has 19 land cover classes from which eight classes were considered in this study. The dominant landscape types considered (see Table S5) in the sub-grid discretization were alpine regions (rock outcrops), glaciers, grasses and shrubs, water bodies, wetlands, needle leaf forest, mixed forest, and broadleaf forest (Figure 4). This discretization resulted in 15,929 tiles (mapping GRUs to grid cells) across the entire domain. The soil column was discretized into four layers, with thicknesses 0.10, 0.25, 1.65, and 2.00 m increasing from top to bottom. LSM calculations are made at the tile level while routing moves the flow between grid cells.

High resolution RDPS and CaPA (2.5 km) have been available only since 2018 and thus could be used for forecasting but not for model development. The sparsity of station data in the region means there is little advantage in using the higher resolution over the 10 km resolution, especially when considering the additional download and

processing load. Model resolution was thus selected to match the resolution of the input forcing data used for model development, considering issues around routing between grid cells, and computational time. The sparse assimilation of surface observations in this remote region means that 10 km is a reasonable resolution of the MESH model configuration for such a large domain.

Given the detailed calculation required in resolving energy and water budget components, CLASS requires seven meteorological forcing inputs outlined in Table 2. Meteorological forcing data were extracted at the resolution of 0.125° (~10 km) from the Regional Deterministic Prediction System (RDPS) and the Global Deterministic Prediction System (GDPS) products of the Global Environmental Multiscale (GEM; Côté et al., 1998) numerical weather model that is currently maintained operationally by Environment and Climate Change Canada (ECCC). The Canadian Precipitation Analysis (CaPA; Mahfouf et al., 2007) was used as the most reliable available dataset to replace GEM precipitation in hindcast mode and for historical calibration and validation simulations during model development. CaPA is an operational product that combines precipitation observations (i.e., stations, and more recently radar) with a background field obtained from the short-term RDPS to produce a near real-time six hourly analysis (Lespinas et al., 2015). The use of GEM predictions as a background partly accounts for topographic information. Strict quality control procedures are used to avoid the assimilation of biased

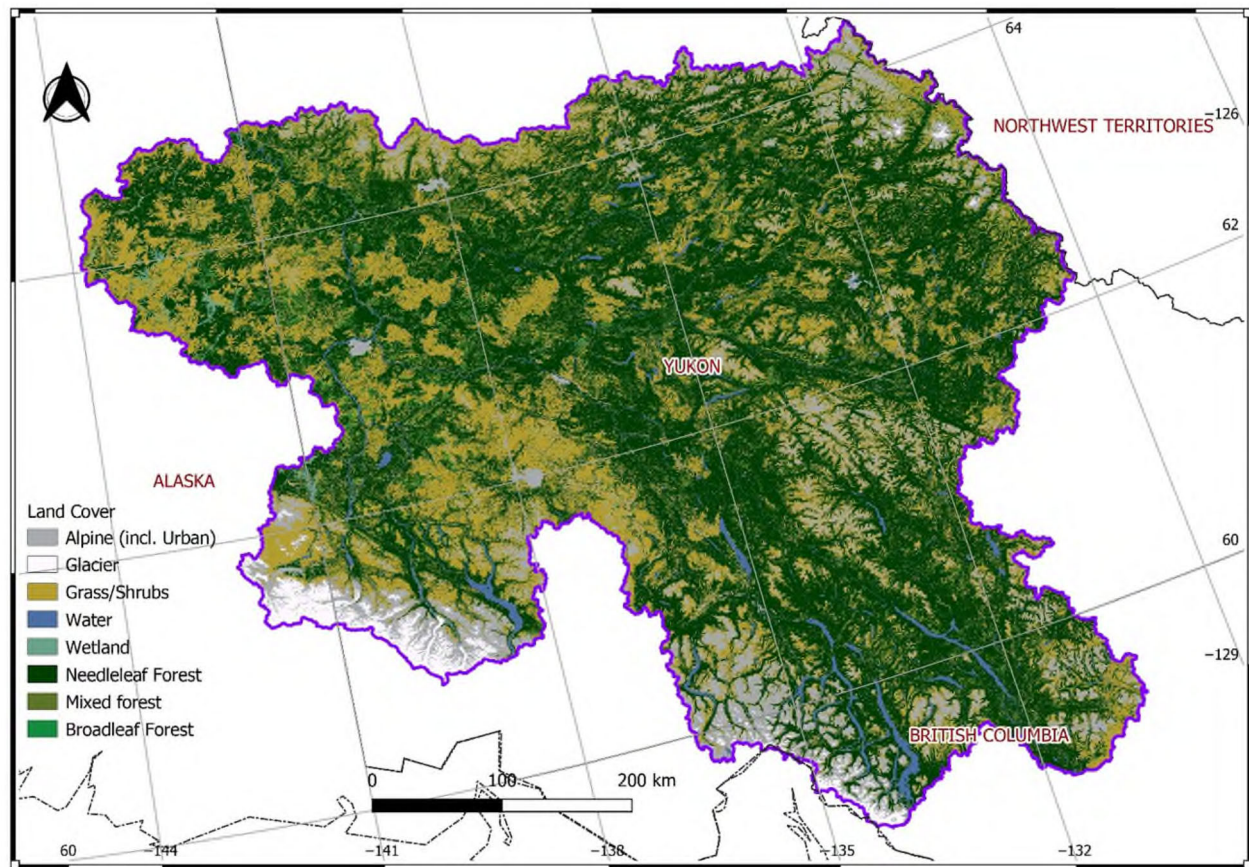


FIGURE 4 Land cover data for the YRB@Eagle based on 2010 NALC LANDSAT 30 m dataset.

TABLE 2 Meteorological variables used in MESH

Variable	Units	Height
Incoming shortwave radiation	$W m^{-2}$	Surface
Incoming longwave radiation	$W m^{-2}$	Surface
Total precipitation rate (CaPA)	$kg m^{-2} s^{-1}$	Surface
Air temperature	K	40 m
Wind speed	$m s^{-1}$	40 m
Barometric pressure	Pa	Surface
Specific humidity	$kg kg^{-1}$	40 m

observations, and in particular wind-induced undercatch of solid precipitation which is detected and handled using temperature and wind speed analysis (Gasset et al., 2021).

3.2 | Model parameterization

The next step in model development was to populate the parameters with appropriate values to replicate the water budget at the designated forecast points while

maintaining an acceptable degree of model fidelity, based on the physical understanding of the basin. Validation of basin states and fluxes (e.g., snow depth or SWE, evapotranspiration, soil moisture, etc.) could be performed using limited available data from research sites. For example, correlation analysis between accumulated winter precipitation (from CaPA) and May 1st snow surveys from Yukon Environment was conducted for the Klondike sub-basin and showed discrepancies in CaPA precipitation from 1 year to another. It was found that when the agreement between CaPA accumulated snow and May 1st snow survey at Midnight Dome site (09EB-SC01) is not good, the model is unable to capture the spring freshet due to errors in input precipitation. For example, the model underestimated the peak flow of 2013 and overestimated it in 2010 and this was due to underestimation and overestimation of winter snow accumulation by CaPA in those 2 years, respectively. The MESH GRU approach is largely landscape-based, which permitted parameter transfers across large regions as demonstrated by Dornes et al. (2008) who transferred tundra parameters in CLASS over 1000 km from Wolf Creek Research Basin in southern Yukon to Trail Valley Creek Research Basin in the Northwest Territories.

The model requires several types of parameters for vegetation, soil, and routing as explained in Section S1. Vegetation parameters are usually obtained from literature and previous studies in the basin, but some are calibrated. Soil hydraulic and thermal parameters are typically estimated from soil texture information. Soil texture parameters were grouped by GRU in accordance with the ecotypes typically found in the Yukon basin where soil types, vegetation types, and permafrost characteristics often coincide. The Global Soil Database for Earth system modeling (GSDE; Shangguan et al., 2014) provided guidance on soil texture parameter ranges and final values were calibrated due to inconsistencies in this database across national borders and the uncertainty in soil for regions such as Yukon where soil surveys are sparse to non-existent.

For the current study, streamflow records were used to calibrate a selected set of sensitive parameters while other parameters were transferred from previous studies on other basins. To maximize the utility of streamflow gauge records available in the basin, and to inform the calibration process, the period 2004–2015 was selected for analysis of discharge based on the concurrent availability of flow records and climatic forcing. The analysis (Section S2.1) resulted in a total of 25 usable streamflow gauges and indicated the important source sub-basins as well as those with very little contribution.

The calibration strategy proceeded initially in two stages; water balance parameters were first calibrated for dominant GRUs to minimize volume balance errors at the 25 stations (Section S2.2); then routing parameters for stream channels, overland flow and baseflow components were calibrated to maximize the sum of NSE (Section S2.3). The 2004–2015 record was split into two periods: 2004–2011 and 2012–2015 used as calibration and validation periods, respectively. We used a split-sample ratio of 2:1 to have enough data for calibration

and used them in series to avoid issues with initialization. The two periods do not exhibit large differences in terms of climate or streamflow except that 2013, which is included in the validation period, was a high flow year for most sub-basins. The parameter set selected for calibration was limited to a subset of what Haghnegahdar et al. (2017) listed in their analysis as the most sensitive parameters. In both stages, calibration was performed using the Dynamically Dimensioned Search (DDS; Tolson & Shoemaker, 2007) optimization algorithm with 5000 iterations and metrics were calculated based on incremental sub-basin runoff contributions to avoid overweighing downstream sub-basins over upstream ones). Five river classes were created to increase the degrees of freedom when calibrating the routing parameters as explained in Section S2.3.

Due to remaining water balance errors affecting the glacier-fed southern sub-basins (Atlin, Upper White, and Kluane), hard-coded glacier albedo in CLASS had to be adjusted as described in Section S2.4. The basin also includes several important lakes which control streamflow through changes in storage, specifically in Teslin, Yukon Headwaters, Takhini, and White River sub-basins. These were integrated in the model setup (drainage database) as routing elements and storage-outflow relationships for a set of lakes were developed (Section S2.5). The parameterization process was iterative. After adjusting the glacier albedo and calibrating lake outflow relationships, additional fine-tuning runs were executed to re-optimize parameters further considering those changes.

3.3 | Model performance assessment

All eight forecast points in the basin, except 09EB001 (Yukon River at Dawson), had flow records for the selected calibration/validation periods with minimal

TABLE 3 Designated forecast points

Station ID	Station name	Sub-basin	Area (km ²)
09AB001	Yukon River at Whitehorse	Yukon Headwaters	19,552
09BA001	Ross River at Ross River	Pelly River	7306
09BC002 ^a	Pelly River at Ross River	Pelly River	18,400
09BC001	Pelly River at Pelly Crossing	Pelly River	48,867
09CB001	White River at Km 1881.6 Alaska Highway	White River	6233
09DC006 ^a	Stewart River near Mayo	Stewart River	31,600
09DD003	Stewart River at The Mouth	Stewart River	51,023
09EA003	Klondike River above Bonanza Creek	Klondike River	7814
09EB001	Yukon River at Dawson	Yukon Main Stem	264,000
09ED001	Yukon River at Eagle	Yukon Main Stem	288,071

^aSecondary forecast points not used for validation (recent discharge records are not available).

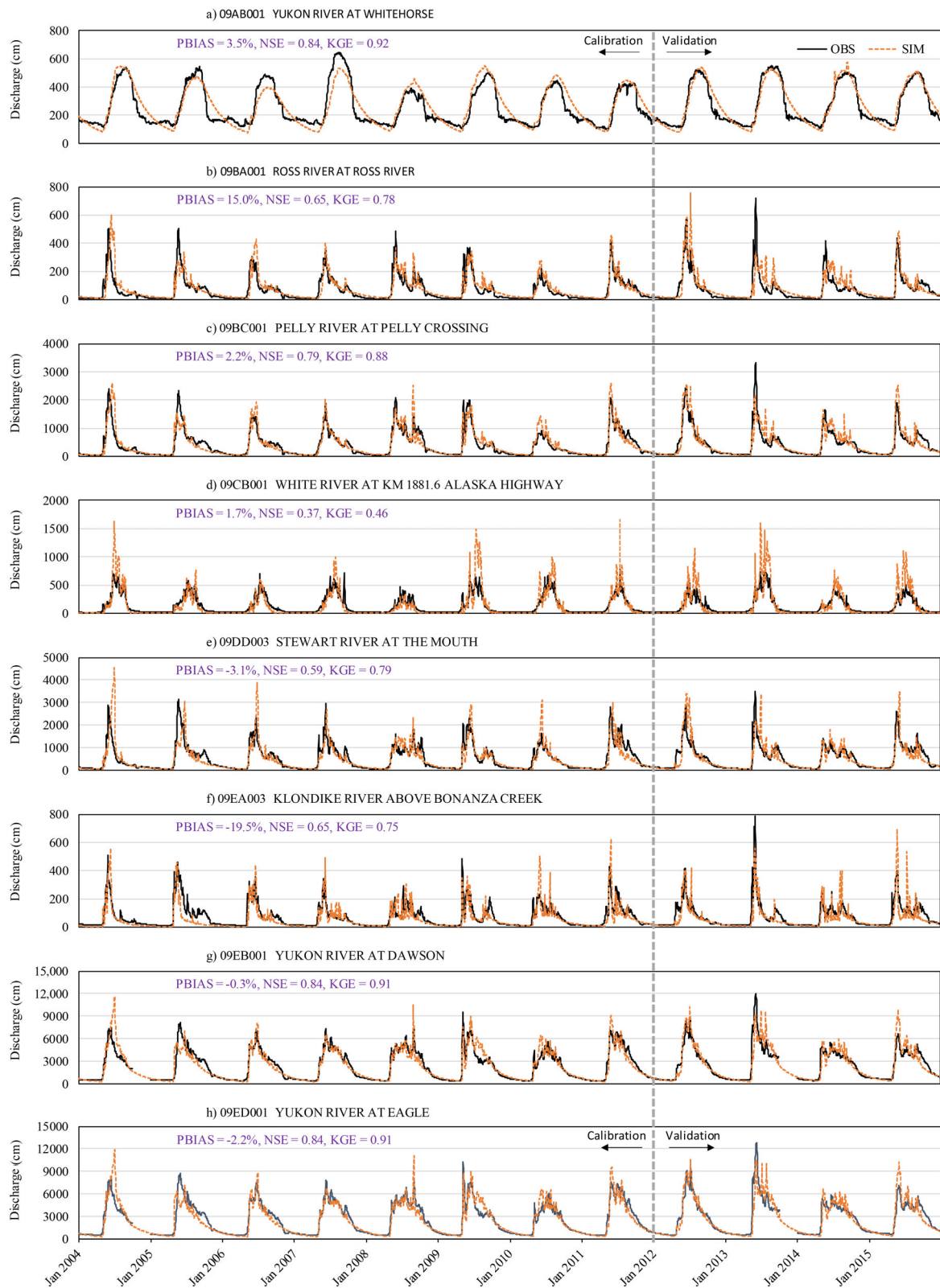


FIGURE 5 Hydrographs at main forecast points over the 2004–2015 period, the vertical dashed gray line separates the calibration and validation periods (2004–2011 and 2012–2015, respectively). Metrics shown are for the whole period.

gaps. Gaps were skipped when calculating performance metrics. To evaluate the model at 09EB001, a flow record was reconstituted in two steps: (1) an open water rating

curve was constructed from concurrent level and flow records (1960–1976) and used to extend the flow record until mid-1996 when water level records at Dawson

TABLE 4 Performance at main forecast points for calibration, validation, whole period and median of annual values over the whole period (metrics calculated individually for each year)

Forecast point	Calibration: 2004–2011			Validation: 2012–2015			Overall: 2004–2015			Median of annual values		
	NSE	KGE	PBIAS	NSE	KGE	PBIAS	NSE	KGE	PBIAS	NSE	KGE	PBIAS
09AB001	0.81	0.90	3.8%	0.90	0.94	3.0%	0.84	0.92	3.5%	0.84	0.85	4.7%
09BA001	0.67	0.79	14.1%	0.63	0.76	16.7%	0.65	0.78	15.0%	0.74	0.73	15.6%
09BC001	0.79	0.89	0.4%	0.78	0.87	5.4%	0.79	0.88	2.2%	0.77	0.79	2.4%
09CB001	0.47	0.56	−7.9%	0.13	0.21	16.7%	0.37	0.46	1.7%	0.57	0.43	3.1%
09DD003	0.56	0.78	−3.4%	0.66	0.81	−2.5%	0.59	0.79	−3.1%	0.70	0.79	1.0%
09EA003	0.64	0.74	−20.3%	0.66	0.76	−18.2%	0.65	0.75	−19.5%	0.62	0.71	−16.5%
09EB001	0.83	0.91	−1.6%	0.83	0.89	1.9%	0.83	0.91	−0.3%	0.84	0.86	0.3%
09ED001	0.84	0.91	−3.4%	0.84	0.90	0.1%	0.84	0.91	−2.2%	0.85	0.88	−1.5%

stopped; (2) a correlation between open water flows at Dawson and Eagle was established for the period 1983–1996 and applied to extend the record at Dawson until 2016. Water level measurements at Dawson were resumed in 2014 and the establishment of an updated rating curve there would further improve flow estimates at Dawson.

Figure 5 shows streamflow hydrographs for main forecast points (Figure 2; Table 3) during the calibration and validation period, which visualizes model performance in all simulation aspects (low and high flow, timing, and volume). Table 4 summarizes NSE and PBIAS over the calibration, validation, and lumped periods. Biases are acceptable (below 10%) for all gauges except for Ross and Klondike Rivers with 15% and −19.5% (overall). The model performance is satisfactory for forecast points on the main Yukon River stem for most years and does not drastically deteriorate when moving to the validation period. The representation of sizable lakes in the model and the parameterization of glacier albedo helped attain good simulation results at Whitehorse, which propagated downstream at Dawson and Eagle with $NSE > 0.80$. At the Ross River forecast point (09BA001), the results are acceptable but vary in quality from 1 year to another (overall $NSE = 0.65$). The impact of this behavior is alleviated to some extent downstream at the Pelly River outlet (09BC001), which is satisfactory for most years ($NSE = 0.79$). The simulation performance of the Klondike River (09EA003) is moderate ($NSE = 0.62$) while the lowest overall NSE (0.37) was found for the Upper White River (09CB001), where the model tends to overestimate peaks. This is likely due to the uncertain accuracy of the forcing meteorology over high mountains, the occurrence of glacial lake outbursts and melt of ice-cored moraine, and the presence of small water bodies that could not be resolved within the large-scale modeling framework here. The lack of high

elevation weather stations and detailed hydrological studies in much of the glaciated headwaters prevented a diagnostic assessment of model performance beyond streamflow.

As the ultimate purpose of this modeling exercise is to provide hydrological forecasts to Yukon Environment, daily peak flows and their days of occurrence were also compared with observations at the main forecast points (Figure 6). The performance was satisfactory especially for the main stem. Three main factors hampering modeling performance here could be noted: the poor quality of the CaPA product due to scarce or non-existent precipitation observations to assimilate within some sub-basins and at high elevations (see Figure 1); the use of a relatively coarse grid which clearly affected solutions at sub-basins having smaller areas, such as the Klondike River, where representing the detailed river network becomes essential and in high mountains where coarse grids do not reflect actual topography and hence orographic effects on precipitation; and the uncertain hydrological behavior of numerous sub-grid lakes and wetlands in the YRB system, and thus their rough consideration through calibration.

4 | FORECASTING SYSTEM OPERATION AND ASSESSMENT

A cloud-based automated hydrological forecasting system that accommodates and operationalizes the YRB@Eagle MESH model was established in a real-time forecasting mode. The established workflow comprises a set of scripts to prepare the meteorological forcing data and then MESH models run for several model setups according to a few configuration files. The model setups were prepared and organized in separate folders and provide streamflow forecasts at designated forecast points

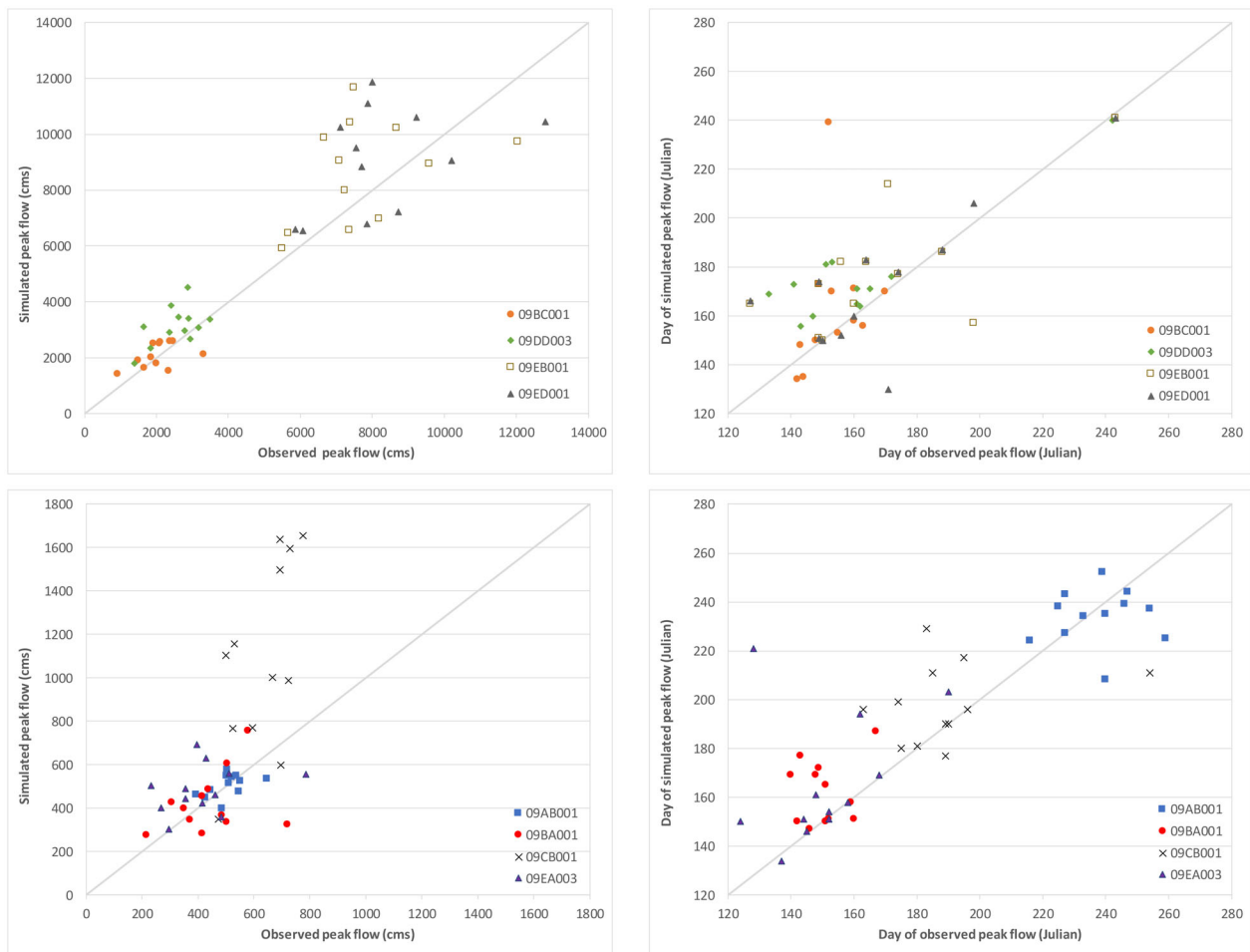


FIGURE 6 Performance of hydrological model for annual daily peak values and timing over the period 2004–2015 for main forecast points. Stations were grouped based on their peak flow values for better scaling.

(Table 3). This workflow relies on a few configuration files that provide details about data files to download, model setups to run, and stations to generate the forecasts at. These facilitate the addition of forecast points and/or model setups (e.g., at higher resolution for a sub-basin or using a different set of parameters). These also allow porting the system to other basins once models are developed for those following the detailed recipe presented in Section 2. Data and computations are hosted on the Amazon Elastic Compute Cloud (EC2) provided by Amazon Web Services (AWS).

4.1 | Forecasting workflow

One forecasting cycle consists of a CaPA hindcast and two GEM forecasts using the MESH system (Figure 7). The 24-h CaPA hindcast, from 16:00 PST 2 days before the day of forecast, updates hydrologic states using CaPA precipitation data (which assimilates atmospheric observations as available) and RDPS forecast data for other

variables. A 48-h RDPS forecast follows and starts from 16:00 PST 1 day before the day of forecast and extends until 16:00 PST the day after the day of forecast. A 10-day GDPS forecast starts at 16:00 PST 1 day before the day of the forecast and extends for 234 h (10 days minus 6 h) until 07:00 PST, 9 days after the forecast day. Given that the GDPS run starts at 16:00 on the day before the forecast issue, and the forecast is issued on the day of the forecast (at 07:00 PST), the actual lead time is about 9 days.

The workflow (Figure 8) starts by downloading ECCC GDPS and RDPS forecast data and CaPA data from ECCC datamart (<https://dd.meteo.gc.ca/> or <http://hpfx.collab.science.gc.ca/>). Meteorological forcing data for each model setup is then prepared from these datasets and stored. The MESH model is run as mentioned above to produce discharges for the locations specified corresponding to hydrometric stations for which observed data is also downloaded. Finally, a set of R scripts post-process the MESH output and generate the required plots. The workflow is automated in four stages that are scheduled

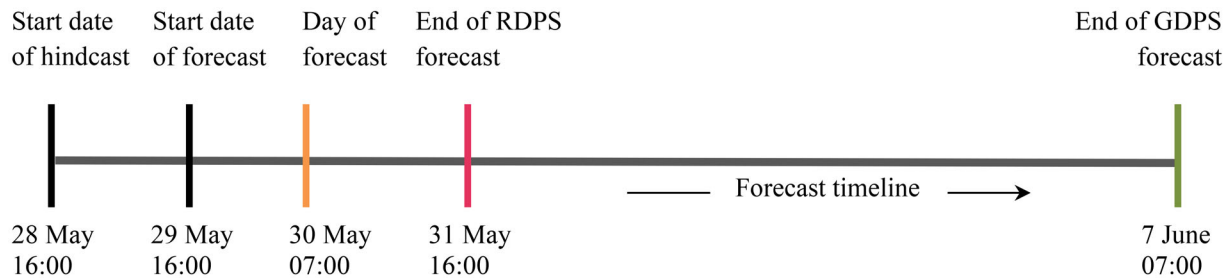


FIGURE 7 Sketch of forecast timeline with an example of dates/times.

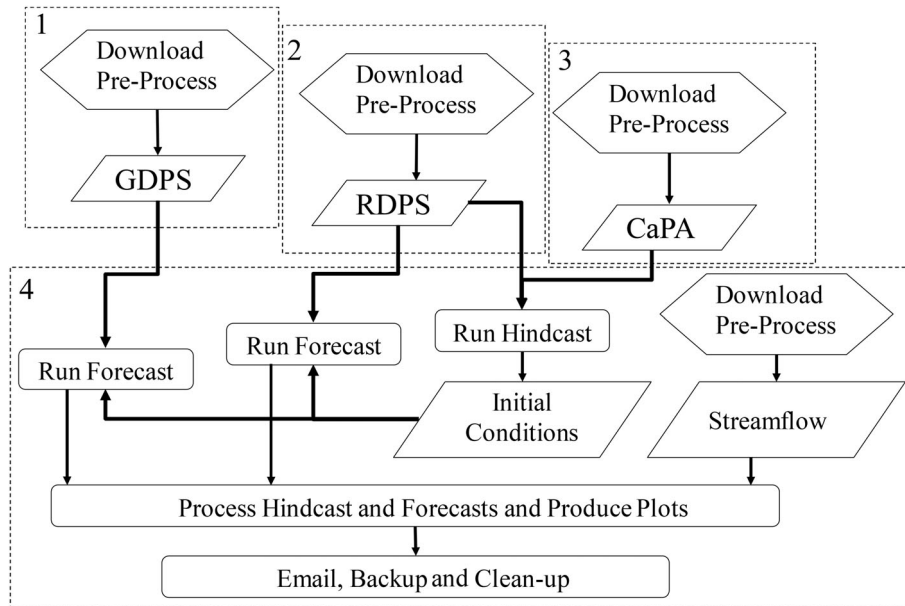


FIGURE 8 Forecast system workflow.

at different times to download the data as soon as they become available. Provisions are made such that stages 1 and 2 can run in parallel; but are also attempted several times in case of server or communication issues. Model simulations (stage 4) cannot start unless all forcing data (CaPA, RDPS and GDPS) have been downloaded and pre-processed. This is a simple proof-of-concept workflow based on scripts and can benefit in the long run from a more robust forecasting scheduling system. The forecasting workflow and the 10 km YRB@Eagle model configuration are available at: <https://github.com/MESH-Model/Yukon-Forecasting-System>.

The current workflow has a total of nine model setups: the YRB@Eagle, described in Section 2, four setups constructed for four separate sub-basins at 5 km resolution, and four other sub-basin setups produced during the 2018–2019 initial stage of the project (Table 5). With the aid of configuration files, streamflow plots are produced to include all forecasts produced for a designated station showing a small multimodel ensemble. In the future, this will help assess the forecasting skill of hydrological setups with differing parameterizations and ensure flexibility in managing

the core of the forecast support system in terms of updates and addition/retirement of setups.

In terms of computational load, the system uses one virtual processor on the AWS cloud and requires about 70 min of wall-clock time to download and process GDPS data for the nine model configurations (Stage 1—refer to Figure 8). RDPS processing (Stage 2) requires about 15 min of wall-clock-time while other downloading/processing (Stage 3) is negligible. Running the models (Stage 4) and producing the final outputs requires around 25 min. Thus, in total, one cycle of the workflow requires about 2 h of run-time distributed throughout the day. However, these processing times are achieved during optimal operation of the workflow, when all data are readily available on time. The cloud-based scripts allow for redundancy and data checks in the system, specifically to deal with missing meteorological forecasts or periods of poor connectivity, minimizing user intervention. In these cases, run times can be longer.

An example showing the end result of the workflow is shown in Figure 9 and displays gauged and modeled discharge for the Yukon River at Dawson, as well as

TABLE 5 Details of current model setups within the forecast system—See Table 3 for forecast points

Model setup	Resolution	Description
YRB@Eagle	0.125° ~10 km	Sections 2 and 3, referred to as 10 K on forecast charts, produces forecasts at all forecast points
Klondike	0.0625° ~5 km	Klondike 5 K, produces forecast at station 09EA003
White		White 5 K, produces forecast at station 09CB001
Pelly		Pelly 5 K, produces forecast at stations 09BA001 and 09BC001
Stewart		Stewart 5 K, produces forecast at station 09DD003
Yukon Headwaters	0.125° ~10 km	Developed during the pilot phase (2018–2019), denoted 10 K-old, produces forecast at station 09AB001
Pelly@Ross		Developed during the pilot phase (2018–2019), denoted 10 K-old, produces forecast at stations 09BA001 and 09BC002
Stewart@Mayo		Developed during the pilot phase (2018–2019), denoted 10 K-old, produces forecast at station 09DC006
Upper Liard ^a		Developed during the pilot phase (2018–2019), denoted 10 K-old, produces forecast at station 10AA001 (Liard River at Upper Crossing) ^a

^aAdditional forecast point in a different basin—not listed in Table 3.

precipitation, evapotranspiration, snowpack and soil moisture from the basin average water balance. Typically, a hindcast period of 15 days is shown together with the forecasts. The content and appearance of the plots are designed to provide a comprehensible, informative, and visually clear forecast information. Daily forecast support emails are automatically sent to a predefined list of recipients every morning. Crude streamflow nudging is used to align the forecast at its start to the most recent streamflow observation and is extended to the hindcast.

4.2 | Preliminary evaluation of the forecast system

The system has been run for the forecast seasons 2020 and 2021, which start mid-April and end mid-October. A

preliminary version of the system was also established and run in 2018 and 2019 as an initial test program. The assessment presented below focuses on the workflow established starting in 2020. During that period, the system required minimal manual intervention to overcome nine failure occurrences in 2020, where the system could not complete the workflow on time. These failures were mostly a result of inability to download the meteorological forcing data due to production delays or connectivity issues, but the forecast was usually still issued later that same day. Failures were analyzed and used to increase the robustness of the system and thus 2021 recorded only two failures.

To illustrate the system usefulness in operational forecast setting, three performance examples linked to 2020 summer storms over the basin combined with high altitude snow/ice melt are reported here. The first event involves the prediction of a critical high-water situation in the Klondike sub-basin and at its forecasting point, which put the community of Rock Creek under alert (CBC News, 2020). Two models (10 K and 5 K Klondike—see Table 5) consistently forecasted high peak discharges from June 17. Figure 10a displays the forecast of June 18 where forecasts from both the 10 and 5 km models indicated peak flows close to $500 \text{ m}^3 \text{ s}^{-1}$ to be expected on June 24 and 26, respectively. These signals informed Yukon Environment flood forecasters, and they initiated the flood response preparedness plan for vulnerable populated areas and infrastructure. Actual discharge peaked at around $662 \text{ m}^3 \text{ s}^{-1}$ on June 23, as shown in Figure 10b, where the hindcast demonstrated the ability of the 10 km model to reproduce the peak flow for this event and indicated that routing parameters' adjustment was required for the 5 km model to improve the timing of its forecast. In contrast, the failure of both models to simulate the two preceding peaks of lower magnitude was due to excessive smoothing by meteorological forecasts and CaPA of two corresponding precipitation events when amounts were compared with hourly observations from Dawson Auto and Klondike FC stations downloaded from Yukon's Road Weather Information System (RIWS, 2020).

The second example depicts how the forecasting system successfully estimated high flows for the White River forecasting point (09CB001) in operational mode even though our model analysis did show difficulties stemming largely from a macrepresentation of its glacial hydrology. While the bridge at 1881.6 km Alaska Highway is relatively safe from historically recognized high water levels, sudden changes of river flows and levels remain a danger for communities, encampments and those fishing and canoeing, especially in late summer. The system forecasted high peak flows starting August

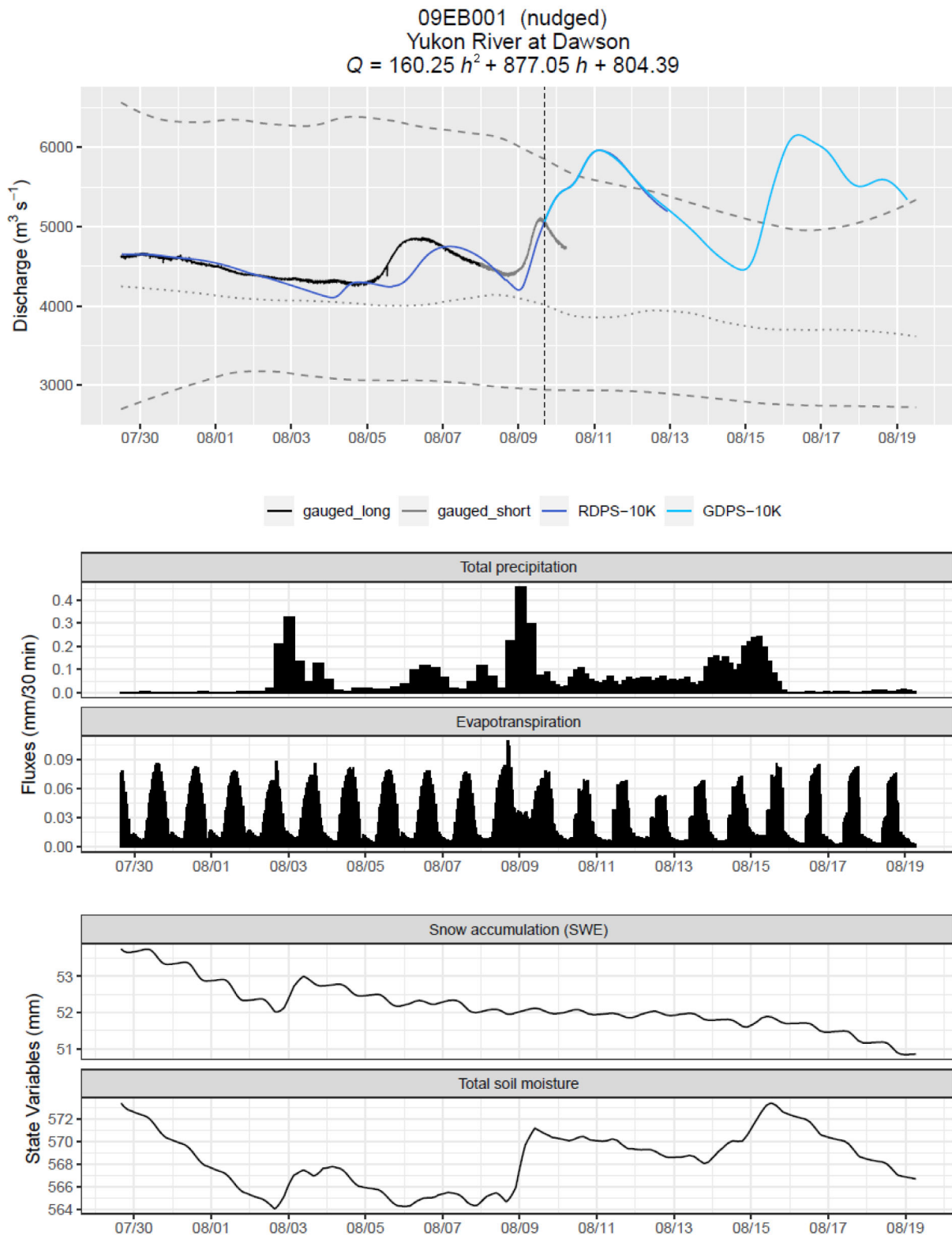


FIGURE 9 Example forecast plots for station 09EB001 issued on August 10, 2021. The top panel shows hourly streamflow forecast, hindcast and available observations as well as long-term (1945–1976) maximum, minimum, and median flows for the plotted period (dashed and dotted lines). The vertical dashed line indicates the start of the forecast. The 10 K refers to the YRB@Eagle model setup with prefixes RDPS and GSPS indicating the meteorological forcing. The water balance plots show the evolution of two meteorological fluxes: Evapotranspiration (model output) and precipitation (input), and two modeled state variables: Snowpack and soil total moisture as averages at the basin level.

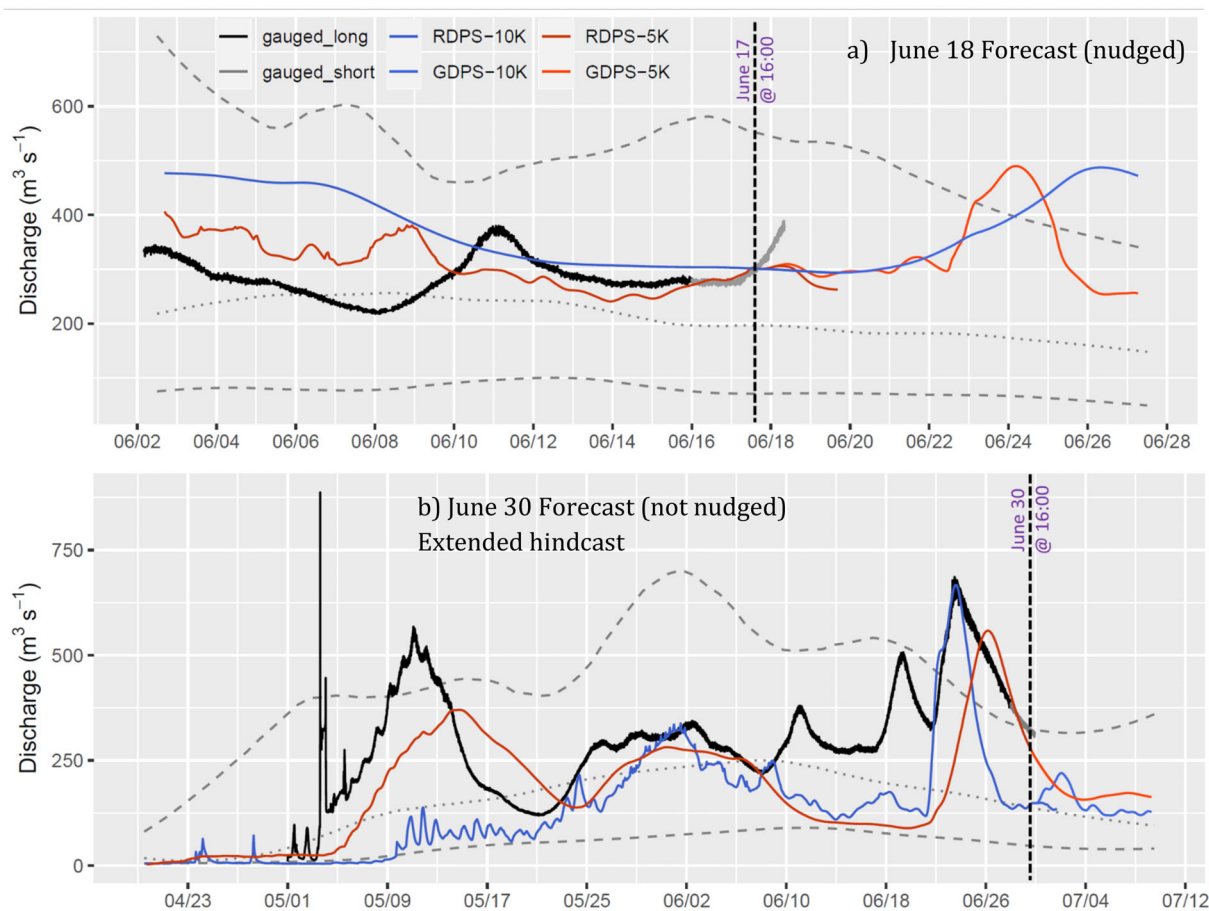


FIGURE 10 Forecasts issued for the Klondike River above Bonanza Creek (09EA003) on (a) June 18 and (b) June 30 with a longer hindcast period. The dashed lines represent historic (1965–2017) recorded minimum and maximum for each day while the dotted line shows median daily flows for each day.

9 and getting higher over the week. On August 11 (Figure 11a), peak flow forecast for August 15 of 620 and 700 m³ s⁻¹ were predicted by the 10 K and 5 K models. Much higher flows materialized on August 14 causing the failure of the gauge. Disruption and afterward WSC determined the actual peak discharge to be 1490 m³ s⁻¹. The models were run in hindcast mode producing 1050 and 1175 m³ s⁻¹ for the flood peaks by the 10 K and 5 K models, respectively (Figure 11b).

A demonstration for Dawson City is displayed in the forecast of August 9, 2020 (Figure 12). The system's YRB@Eagle model forecasted flow increasing from around 4840 to 6500 m³ s⁻¹ by August 18, whereas the later observed crest reached 6000 m³ s⁻¹ on August 19. These late summer high-flow events are very difficult to predict since they involve a combination of forecasted rainfall and high-elevation snowpack/glacier melt. Again, this model skill provided guidance on quickly changing conditions allowing the authorities some lead-time in releasing governmental high-water advisories, flood watches, or flood warnings.

5 | CONCLUSIONS AND FUTURE DEVELOPMENT NEEDS

A streamflow forecast support system was developed to provide operational forecasts of streamflow and water balance for the sparsely monitored YRB in the Yukon Territory, Canada. This basin is 119% of the area of the United Kingdom yet has only 25 streamflow gauges available for model calibration and verification. The MESH model was used to simulate the hydrology of this basin on a continuous basis with good success. A process-oriented approach to the real modeling constraints in this region, demonstrated that an epistemic physically based process hydrology methodology combined with some traditional modeling approaches provided a good compromise and reasonable guidance around high flow events. Despite the detailed physical representation and parameter selection from hydrology research in the region, some model parameter calibration was still necessary in reaching acceptable streamflow simulation results. The scarcity or absence of meteorological and hydrometric

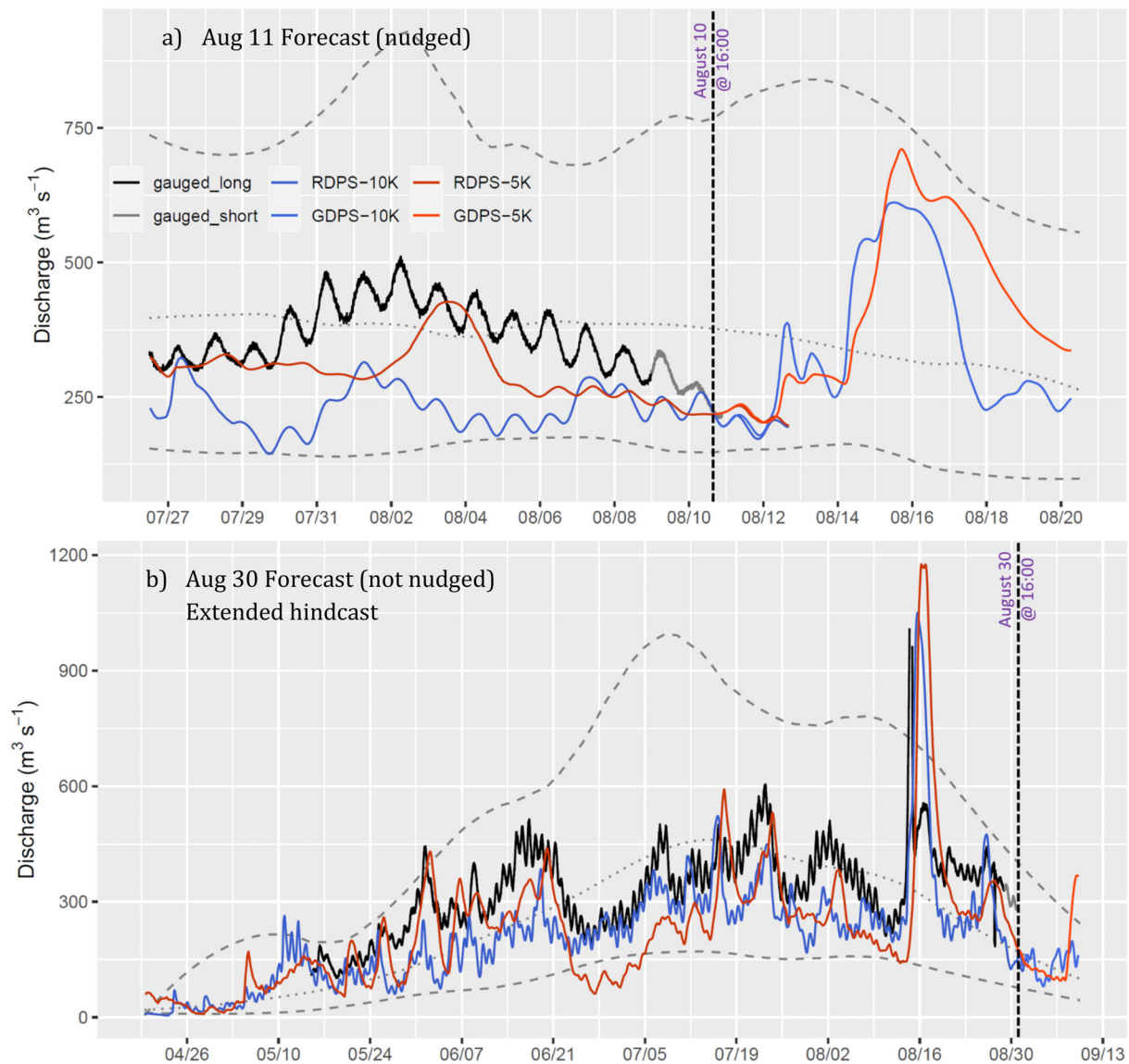


FIGURE 11 Forecasts issued for the White River at km 1881.6 Alaska Highway (09CB001) on (a) August 11 and (b) August 31 with a longer hindcast period. The dashed lines represent historic (1974–2017) recorded minimum and maximum for each day while the dotted line shows median daily flows for each day.

observations in the YRB sub-basins limited the accuracy of the streamflow predictions especially for the remote upper White River which drains extensive icefields. In many instances, there was no correlation between CaPA accumulated winter precipitation and Yukon Environment's snow survey observations, highlighting the highly variable and complex nature of snow representation in this complex terrain.

In the operational forecast support mode, MESH was driven by the ECCC's GEM-CaPA, RDPS, and GDPS to provide hindcasts, and 2- and 9-day forecasts, respectively. The forecasting system platform was coded in-house, hosted in the Amazon Web Service and is quasi-autonomous requiring minimal initialization before the

onset of the melt. So far, 2 years (2020–2021) of operation as an information product for flood forecasting by Yukon Environment concretized an instructive experience in communicating and applying hydrological science advances to support disaster prevention and management at the provincial/territorial level in Canada. Although the amplitude/timing of forecasted flows was not always perfect and a simple shift was applied using crude nudging to observed discharge, the system often recognized flow peaks and their timings well. In some critical situations, Yukon hydrologists were able to add value to this forecast guidance because of their access to local meteorological observation networks, mainly by comparing CaPA to actual precipitation. Thus, additional observations from

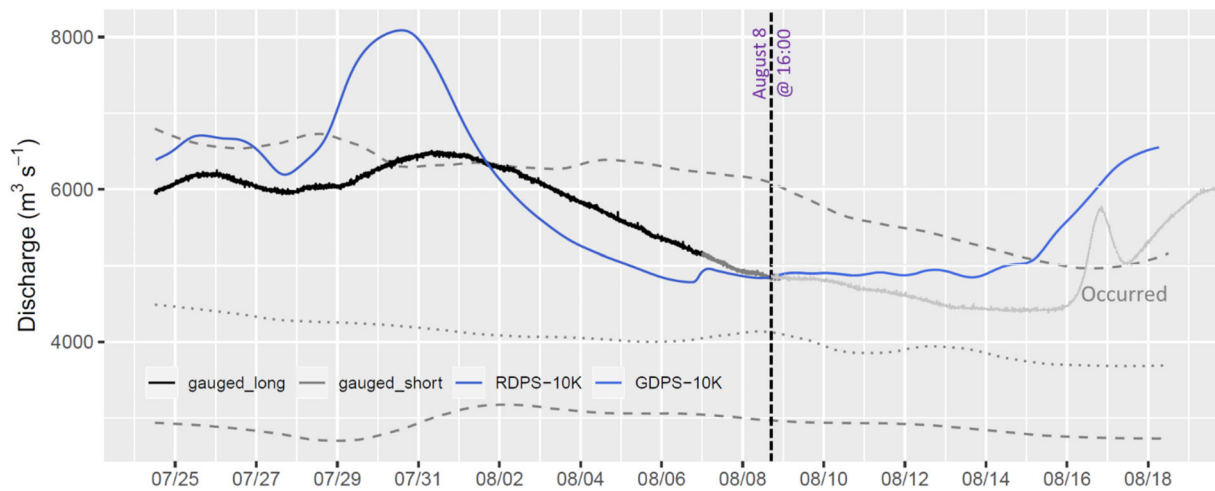


FIGURE 12 Forecast system performance compared with observed streamflow for the Yukon River at Dawson (09EB001). Forecast issued on August 9, 2020, with observations until August 20 superimposed in light gray. The dashed lines represent historic (1945–1980) recorded minimum and maximum for each day while the dotted line shows median daily flows for each day.

Yukon and Alaska local/regional networks ingested into CaPA will likely improve hydrological forecast quality.

The system provides a limited multimodel ensemble forecast but it can be easily extended to use the meteorological ensembles of ECCG GEM to provide an ensemble prediction. The system can also benefit from higher resolution and longer lead times that ECCG GEM is offering for its GDPS and CaPA products. Introducing data assimilation for initial snow states and ongoing streamflow observations can also improve the realism of model prediction. Ongoing MESH model research targeting permafrost (e.g., Elshamy et al., 2020) and glacier descriptions is also expected to enhance prediction reliability. The outputs of the hydrological models can be used to predict ice-jam floods as done for the Athabasca River basin by Lindenschmidt et al. (2019). The current flexibility of the system allows the incorporation of new features efficiently shortening the time to bring research into operation in ungauged basins. The experience of creating this system will inform future research to operation improvements as Canada develops a nationally coordinated flood forecast system. The system serves as a prototype that can be adopted to other basins and regions. The detailed model development and the portable forecasting workflows presented provide a recipe to conduct such tasks and fills a gap for cold basins with sparse observations.

ACKNOWLEDGMENTS


The authors would like to acknowledge the discussion, feedback and support of Heather Jirousek, Holly Goulding, Anthony Bier, Richard Janowicz, and Benoit Turcotte of the Water Resources Branch, Yukon Environment in the development of this system. We also

acknowledge the contributions of Arcadio Rodriguez and Bruce Davison to the early versions of the forecast system. We thank Yukon Environment and the Canada First Research Excellence Fund's Global Water Futures program for funding this project. The cooperation and assistance from Environment and Climate Change Canada were an important contribution to this research. A forecast system would not be possible without ECCG weather and hydrometric stations and MSC weather forecasts. This article is dedicated to the late J. Richard Janowicz, senior hydrologist, and river forecaster for Yukon Environment and before that, DIAND; his encouragement, vision and advice led to the development of the Yukon streamflow forecast system.

DATA AVAILABILITY STATEMENT

All datasets used are in the public domain and sources are mentioned within the manuscript. MESH code and documentation are available through <https://wiki.usask.ca/display/MESH/MESH+User+Page>. The forecasting workflow and the 10km YRB@Eagle model configuration are available at: <https://github.com/MESH-Model/Yukon-Forecasting-System>.

ORCID

Mohamed Elshamy  <https://orcid.org/0000-0002-3621-0021>

REFERENCES

- Arduino, G., Reggiani, P., & Todini, E. (2005). Recent advances in flood forecasting and flood risk assessment. *Hydrology and Earth System Sciences*, 9(4), 280–284. <https://doi.org/10.5194/hess-9-280-2005>

- Belvederesi, C., Zaghoul, M. S., Achari, G., Gupta, A., Hassan, Q. K., Belvederesi, C., Achari, G., Zaghoul, M., Hassan, Q., & Gupta, A. (2022). Modelling river flow in cold and ungauged regions: A review of the purposes, methods, and challenges, 30(1), 159–173. <https://doi.org/10.1139/Er-2021-0043>
- Brabets, T. P., & Walvoord, M. A. (2009). Trends in streamflow in the Yukon River basin from 1944 to 2005 and the influence of the Pacific decadal oscillation. *Journal of Hydrology*, 371(1-4), 108–119. <https://doi.org/10.1016/j.jhydrol.2009.03.018>
- Brabets, T. P., Wang, B., & Meade, R. H. (2000). Environmental and hydrologic overview of the Yukon River basin, Alaska and Canada. In USGS water-resources investigations report (Vol. 99, Issue 4204).
- Brunner, M. I., Slater, L., Tallaksen, L. M., & Clark, M. (2021). Challenges in modeling and predicting floods and droughts: A review. *Wiley Interdisciplinary Reviews: Water*, 8(3), 1–32. <https://doi.org/10.1002/wat2.1520>
- Bush, E., & Lemmen, D. (Eds.). (2019). *Canada's changing climate report*. Government of Canada.
- Carey, S. K., & Woo, M. K. (2001). Spatial variability of hillslope water balance, Wolf Creek basin. *Hydrological Processes*, 15(16), 3113–3132. <https://doi.org/10.1002/hyp.319>
- CBC News. (2020). Rock Creek residents brace for flooding as Klondike waters rise. <https://www.cbc.ca/news/canada/north/rock-creek-residents-flooding-klondike-1.5624504>
- CCRS, CCMEQ, NRCAN, CAMBIO, CONAFOR, INEGI, & USGS. (2017). *2010 north American land cover at 30 meters, edition 1.0*. Commission for Environmental Cooperation. <http://www.cec.org/nalcms>
- Clark, M. P., Wilby, R. L., Gutmann, E. D., Vano, J. A., Gangopadhyay, S., Wood, A. W., Fowler, H. J., Prudhomme, C., Arnold, J. R., & Brekke, L. D. (2016). Characterizing uncertainty of the hydrologic impacts of climate change. In B. Soden (Ed.), *Current climate change reports* (Vol. 2, pp. 55–64). Springer. <https://doi.org/10.1007/s40641-016-0034-x>
- Côté, J., Gravel, S., Méthot, A., Patoine, A., Roch, M., Staniforth, A., Desmarais, J. G., Gravel, S., Méthot, A., Patoine, A., Roch, M., & Staniforth, A. (1998). The operational CMC-MRB global environmental multiscale (GEM) model. Part I: Design considerations and formulation. *Monthly Weather Review*, 126(6), 1373–1395. [https://doi.org/10.1175/1520-0493\(1998\)126<1373:TOCMGE>2.0.CO;2](https://doi.org/10.1175/1520-0493(1998)126<1373:TOCMGE>2.0.CO;2)
- Dornes, P. F., Tolson, B. A., Davison, B., Pietroniro, A., Pomeroy, J. W., & Marsh, P. (2008). Regionalisation of land surface hydrological model parameters in subarctic and arctic environments. *Physics and Chemistry of the Earth*, 33(17-18), 1081–1089. <https://doi.org/10.1016/J.PCE.2008.07.007>
- Elshamy, M. E., Princz, D., Saprizo-Azuri, G., Abdelhamed, M. S., Pietroniro, A., Wheeler, H. S., & Razavi, S. (2020). On the configuration and initialization of a large-scale hydrological land surface model to represent permafrost. *Hydrology and Earth System Sciences*, 24(1), 349–379. <https://doi.org/10.5194/hess-24-349-2020>
- Gasset, N., Fortin, V., Dimitrijevic, M., Carrera, M., Bilodeau, B., Muncaster, R., Gaborit, É., Roy, G., Pentcheva, N., Bulat, M., Wang, X., Pavlovic, R., Lespinas, F., Khedhaouiria, D., & Mai, J. (2021). A 10 km north American precipitation and land-surface reanalysis based on the GEM atmospheric model. *Hydrology and Earth System Sciences*, 25(9), 4917–4945. <https://doi.org/10.5194/hess-25-4917-2021>
- Gelfan, A. N., & Motovilov, Y. G. (2009). Long-term hydrological forecasting in cold regions: Retrospect, current status and prospect. *Geography Compass*, 3(5), 1841–1864. <https://doi.org/10.1111/J.1749-8198.2009.00256.X>
- Haghnegahdar, A., Razavi, S., Yassin, F., & Wheeler, H. (2017). Multicriteria sensitivity analysis as a diagnostic tool for understanding model behaviour and characterizing model uncertainty. *Hydrological Processes*, 31(25), 4462–4476. <https://doi.org/10.1002/hyp.11358>
- Haghnegahdar, A., Tolson, B. A., Craig, J. R., & Paya, K. T. (2015). Assessing the performance of a semi-distributed hydrological model under various watershed discretization schemes. *Hydrological Processes*, 29(18), 4018–4031. <https://doi.org/10.1002/hyp.10550>
- Janowicz, J. R., Hedstrom, N., Pomeroy, J. W., Granger, R. J., & Carey, S. (2004). Wolf Creek Research Basin water balance studies. *IAHS-AISH Publication*, 290, 195–204.
- Jones, S. H., & Fahl, C. B. (1994). Magnitude and frequency of floods in Alaska and conterminous basins of Canada. In Water-resources investigations report. U.S. Geological Survey. <http://pubs.er.usgs.gov/publication/wri934179>
- Kirchner, J. W. (2006). Getting the right answers for the right reasons: Linking measurements, analyses, and models to advance the science of hydrology. *Water Resources Research*, 42, W03S04. <https://doi.org/10.1029/2005WR004362>
- Kouwen, N. (1988). WATFLOOD: A micro-computer based flood forecasting system based on real-time weather radar. *Canadian Water Resources Journal*, 13(1), 62–77. <https://doi.org/10.4296/cwrj1301062>
- Kouwen, N., Soulis, E. D., Pietroniro, A., Donald, J., & Harrington, R. A. (1993). Grouped response units for distributed hydrologic modeling. *Journal of Water Resources Planning and Management*, 119(3), 289–305. [https://doi.org/10.1061/\(ASCE\)0733-9496\(1993\)119:3\(289\)](https://doi.org/10.1061/(ASCE)0733-9496(1993)119:3(289))
- Lespinas, F., Fortin, V., Roy, G., Rasmussen, P., & Stadnyk, T. (2015). Performance evaluation of the Canadian precipitation analysis (CaPA). *Journal of Hydrometeorology*, 16(5), 2045–2064. <https://doi.org/10.1175/JHM-D-14-0191.1>
- Lindenschmidt, K. E., Rokaya, P., Das, A., Li, Z., & Richard, D. (2019). A novel stochastic modelling approach for operational real-time ice-jam flood forecasting. *Journal of Hydrology*, 575, 381–394. <https://doi.org/10.1016/J.JHYDROL.2019.05.048>
- Mahfouf, J.-F. F., Brasnett, B., & Gagnon, S. (2007). A Canadian precipitation analysis (CaPA) project: Description and preliminary results. *Atmosphere-Ocean*, 45(1), 1–17. <https://doi.org/10.3137/ao.v450101>
- Perera, D., Seidou, O., Agnihotri, J., Rasmy, M., Smakhtin, V., Coulibaly, P., & Mehmood, H. (2019). Flood early warning systems: A review of benefits, challenges and prospects 08. <https://inweh.unu.edu/flood-early-warning-systems-a-review-of-benefits-challenges-and-prospects/>
- Pietroniro, A., Fortin, V., Kouwen, N., Neal, C., Turcotte, R., Davison, B., Verseghy, D., Soulis, E. D., Caldwell, R., Evora, N., & Pellerin, P. (2007). Development of the MESH modelling system for hydrological ensemble forecasting of the Laurentian Great Lakes at the regional scale. *Hydrology and Earth System Sciences*, 11(4), 1279–1294. <https://doi.org/10.5194/hess-11-1279-2007>
- Pietroniro, A., & Soulis, E. D. (2003). A hydrology modelling framework for the Mackenzie GEWEX programme. *Hydrological Processes*, 17(3), 673–676. <https://doi.org/10.1002/hyp.5104>
- Pietroniro, A., Soulis, E. D., Snelgrove, K., & Kouwen, N. (2001). A framework for coupling atmospheric and hydrological models. *IAHS-AISH Publication*, 270, 27–34.

- Pomeroy, J. W., Bewley, D. S., Essery, R. L. H., Hedstrom, N. R., Link, T., Granger, R. J., Sicart, J. E., Ellis, C. R., & Janowicz, J. R. (2006). Shrub tundra snowmelt. *Hydrological Processes*, 20(4), 923–941. <https://doi.org/10.1002/hyp.6124>
- Pomeroy, J. W., Fang, X., Shook, K., & Whitfield, P. H. (2013). Predicting in ungauged basins using physical Principles obtained using the deductive. Inductive and abductive reasoning approach. In J. W. Pomeroy, P. H. Whitfield, & C. Spence (Eds.), *Putting prediction in ungauged basins into practice* (pp. 41–62). Canadian Water Resources Association/International Association of Hydrological Sciences.
- Pomeroy, J. W., & Granger, R. J. (1999). *Wolf Creek Research Basin: Hydrology, ecology, environment*. National Water Research Institute, Environment.
- Pomeroy, J. W., Granger, R. J., Hedstrom, N. R., Gray, D. M., Elliott, J., Pietroniro, A., & Janowicz, J. R. (2004). The process hydrology approach to improving prediction of ungauged basins in Canada. In C. Spence, J. W. Pomeroy, & A. Pietroniro (Eds.), *Prediction in ungauged basins: Approaches for Canada's cold regions* (pp. 67–100). Canadian Water Resources Association.
- Pomeroy, J. W., Gray, D. M., Shook, K. R., Toth, B., Essery, R. L. H., Pietroniro, A., & Hedstrom, N. (1998). An evaluation of snow accumulation and ablation processes for land surface modelling. *Hydrological Processes*, 12(15), 2339–2367. [https://doi.org/10.1002/\(SICI\)1099-1085\(199812\)12:15<2339::AID-HYP800>3.0.CO;2-L](https://doi.org/10.1002/(SICI)1099-1085(199812)12:15<2339::AID-HYP800>3.0.CO;2-L)
- Pomeroy, J. W., MacDonald, M. K., Dornes, P. F., & Armstrong, R. (2016). Water budgets in ecosystems. In E. A. Johnson & Y. E. Martin (Eds.), *Hydrological processes of aquatic and terrestrial ecosystems* (pp. 88–132). Cambridge University Press.
- Rasouli, K., Pomeroy, J. W., & Whitfield, P. H. (2021). The sensitivity of North American mountain basin snow hydrology to changes in air temperature and precipitation. April.
- RIWS. (2020). Yukon's road weather information system. <http://rwis.gov.yk.ca/weather/>
- Shangguan, W., Dai, Y., Duan, Q., Liu, B., & Yuan, H. (2014). A global soil data set for earth system modeling. *Journal of Advances in Modeling Earth Systems*, 6(1), 249–263. <https://doi.org/10.1002/2013MS000293>
- Smith, C. A. S., Meikle, J. C., & Roots, C. F. (Eds.). (2004). *Ecoregions of the Yukon territory: Biophysical properties of Yukon landscapes*. Agriculture and Agri-Food Canada, PARC Technical Bulletin 04-01.
- Soulis, E. D., Snelgrove, K. R., Kouwen, N., Seglenieks, F., & Verseghy, D. L. (2000). Towards closing the vertical water balance in Canadian atmospheric models: Coupling of the land surface scheme class with the distributed hydrological model watflood. *Atmosphere-Ocean*, 38(1), 251–269. <https://doi.org/10.1080/07055900.2000.9649648>
- Tolson, B. A., & Shoemaker, C. A. (2007). Dynamically dimensioned search algorithm for computationally efficient watershed model calibration. *Water Resources Research*, 43, W01413. <https://doi.org/10.1029/2005WR004723>
- Vehvilainen, B., & Huttunen, M. (2001). *Hydrological forecasting and real-time monitoring: The watershed simulation and forecasting system (WSFS)* (pp. 13–20). Finnish Environment Institute. <https://doi.org/10.1002/9780470511121.ch2>
- Verseghy, D. (2012). CLASS—The Canadian land surface scheme (version 3.6)—technical documentation. Internal Report, Climate Research Division, Science and Technology Branch, Environmental Canada, February.
- Wahl, H. E. (2004). Climate. In C. A. S. Smith, J. C. Meikle, & C. F. Roots (Eds.), *Ecoregions of the Yukon territory: Biophysical properties of Yukon landscapes* (pp. 19–23). Agriculture and Agri-Food Canada, PARC Technical Bulletin No. 04-01.
- Wahl, H. E., Fraser, D. B., Harvey, R. C., & Maxwell, J. B. (1987). *Climate of Yukon. Climatological Studies* (Vol. 40). Atmospheric Environment Service, Environment Canada.
- Werner, M., & van Dijk, M. (2005). Developing flood forecasting systems: Examples from the UK, Europe, and Pakistan. In S. Y. Liong, K. K. Phoon, & V. Babovic (Eds.), *Proceedings of the 6th international conference on hydroinformatics* (pp. 1205–1212). World Scientific Publishing Company.
- Wheater, H. S., Pomeroy, J. W., Pietroniro, A., Davison, B., Elshamy, M. E., Yassin, F., Rokaya, P., Fayad, A., Tesemma, Z., Princz, D., Loukili, Y., DeBeer, C., Ireson, A., Razavi, S., Lindenschmidt, K.-E., Elshorbagy, A., MacDonald, M., Abdelhamed, M., Haghnegahdar, A., & Bahrami, A. (2022). Advances in modelling large river basins in cold regions with modélisation environnementale communautaire - surface and hydrology (MESH), the Canadian hydrological land surface scheme. *Hydrological Processes*, 36(4), e14557. <https://doi.org/10.1002/hyp.14557>
- Yamazaki, D., Ikeshima, D., Sosa, J., Bates, P. D., Allen, G. H., & Pavelsky, T. M. (2019). MERIT hydro: A high-resolution global hydrography map based on latest topography dataset. *Water Resources Research*, 55(6), 5053–5073. <https://doi.org/10.1029/2019WR024873>
- Yassin, F., Razavi, S., Wheater, H., Sapriza-Azuri, G., Davison, B., & Pietroniro, A. (2017). Enhanced identification of a hydrologic model using streamflow and satellite water storage data: A multicriteria sensitivity analysis and optimization approach. *Hydrological Processes*, 31(19), 3320–3333. <https://doi.org/10.1002/hyp.11267>
- Yassin, F. (2019). Towards improved hydrologic land surface modelling: enhanced model identification and integration of water management [PhD Thesis, Saskatoon, University of Saskatchewan]. <https://harvest.usask.ca/handle/10388/12398>
- Zahmatkesh, Z., Kumar Jha, S., Coulibaly, P., & Stadnyk, T. (2019). An overview of river flood forecasting procedures in Canadian watersheds. 44(3), 213–229. <https://doi.org/10.1080/07011784.2019.1601598>

SUPPORTING INFORMATION

Additional supporting information can be found online in the Supporting Information section at the end of this article.

How to cite this article: Elshamy, M., Loukili, Y., Pomeroy, J. W., Pietroniro, A., Richard, D., & Princz, D. (2022). Physically based cold regions river flood prediction in data-sparse regions: The Yukon River Basin flow forecasting system. *Journal of Flood Risk Management*, e12835. <https://doi.org/10.1111/jfr3.12835>